

Entanglement generation by vacuum and thermal phonon fields via the optomechanical interaction

Qidong Xu* and M. P. Blencowe†

Department of Physics and Astronomy, Dartmouth College, Hanover, New Hampshire 03755, USA

(Dated: October 27, 2021)

We present exact solutions for the quantum time evolution of two spatially separated, local inductor capacitor (LC) oscillators that are coupled optomechanically to a long elastic strip that functions as a quantum thermal acoustic field bath. We show that the optomechanical coupling leads to entanglement dynamics between the two oscillators in the absence of real (and virtual) photon or phonon exchange, where entanglement emerges periodically regardless of the temperature of the phonon field. The considered model allows for an explicit validation of causality and, as a phonon-photon optomechanical analogue of the graviton-matter coupling, may shed light on the quantum nature of the gravitational field as a generator of entanglement.

Introduction.— Thermal environments have often been invoked to explain the decoherence of a quantum system, thus resulting in the observed classical, macroscopic world [1–4]. However, it is also quite well known that thermal environments can induce entanglement generation when coupled to otherwise independent quantum subsystems under suitable conditions [5–15]; several experimental realizations have been proposed [5, 16–19], with further examples considered in the Ref. [20] review (and references therein).

In this Letter, we investigate the entanglement dynamics of an experimentally feasible model comprising two spatially separated inductor-capacitor (LC) oscillators that are coupled to a long, partially metallized elastic strip via the optomechanical interaction; here, the elastic strip functions as a thermal phonon environment. A field theoretic description of the environment naturally leads to local, *position-dependent* couplings between the oscillators and the field modes. This then allows for an explicit analysis of the causal nature of the entanglement dynamics between the two oscillators arising from the finite elastic wave propagation speed in the elastic strip, analogous to the speed of light in vacuum. Tracing out the elastic strip (phonon) degrees of freedom, we solve *exactly* for the quantum time evolution of the LC oscillators, with particular attention paid to the competing entanglement and dephasing/rephasing dynamics of the LC oscillators.

With the capacitor sizes much smaller than the elastic strip length, the two LC oscillators can also be thought of as variants of the so-called Unruh-DeWitt (UDW) detector [21, 22], with the bare two-level UDW detector replaced by a quantum harmonic oscillator and the usual bilinear coupling between the detector and field replaced by the quadratic-linear optomechanical-type interaction. A consequence of the optomechanical interaction is that there is no real (or virtual) energy/particle exchange between the detectors and the field, and yet entanglement can still be ‘harvested’ from the quantum field vacuum [23–26]. However, we shall see that the entanglement can only form when the two LC oscillators are ‘timelike’ sep-

arated (i.e., causally connected) as opposed to ‘spacelike’ separated with respect to the elastic wave propagation (i.e., phonon) speed. This is to be contrasted with the usual bilinear, two-level UDW detector-field interaction case, where perturbative leading order calculations [24] suggest that entanglement can be ‘harvested’ from the quantum field vacuum even for spacelike separated detectors. For oscillator type detectors with bilinear couplings to the field, nonperturbative methods can be used to solve for the quantum dynamics, although mixed results have been reported in the literature as to whether two inertial, spacelike detectors can be entangled or otherwise [27, 28].

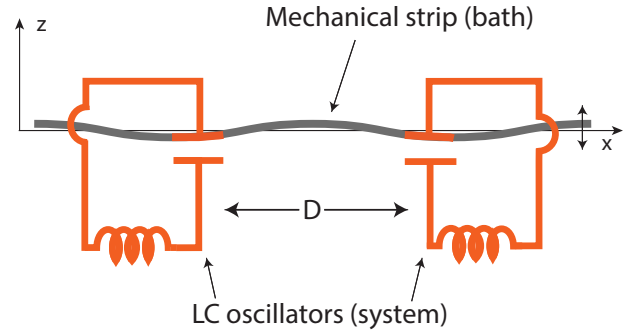


FIG. 1. Scheme of the model system. Two spatially separated LC circuit oscillators (system) are capacitively coupled to a long oscillating, elastic strip (bath) via two metallized segments.

The model.— Our model scheme (Fig. 1) is an extension of one considered in Ref. [29], which investigated dephasing only of a single LC oscillator coupled capacitively to a long elastic strip. In particular, we consider two identical LC circuits separated by a distance D , each coupled capacitively via metallized segment lengths ΔL of a long, elastic mechanical strip with overall length $L > D \gg \Delta L$ that is clamped at both ends. The LC circuits are sited such that the center point between the two capacitors co-

incides with the strip center. The transverse width (W) and thickness (T) of the strip satisfy $T \ll W \ll L$. The indicated lower capacitor plates are assumed fixed, also with length ΔL , the same width W as the strip, and separated from the upper flexing, metallized ΔL strip segments of the strip by a small equilibrium vacuum gap $d \ll W$. The bare, zero flexing capacitance of each LC circuit is then given by the standard parallel plate expression $C_b = \epsilon_0 W \Delta L / d$ with ϵ_0 the vacuum permittivity. In the following we shall denote the left circuit capacitance by C_l and right circuit capacitance by C_r , and we denote both circuit inductances by L .

Neglecting displacements in the transverse y and longitudinal x directions, the flexing mechanical displacement of the strip along the transverse z direction can be described by the Hamiltonian

$$\mathcal{H}_{\text{bath}} = \frac{\rho_m W T}{2} \int_0^L dx \left(\frac{\partial u_z}{\partial t} \right)^2 + \frac{F}{2} \int_0^L dx \left(\frac{\partial u_z}{\partial x} \right)^2, \quad (1)$$

where $u_z(t, x)$ is the displacement field, ρ_m is the mass density of the strip, and we assume a sufficient large tensile force F is applied at both ends of the strip so that it behaves effectively as a string with the boundary conditions $u_z(x=0) = u_z(x=L) = 0$.

The Hamiltonian for the two LC circuit system is

$$\mathcal{H}_{\text{sys}} = \frac{Q_l^2}{2C_l} + \frac{\Phi_l^2}{2L} + \frac{Q_r^2}{2C_r} + \frac{\Phi_r^2}{2L}, \quad (2)$$

where Q_l (Q_r) is the left (right) capacitor charge coordinate and Φ_l (Φ_r) is the left (right) inductor flux coordinate. We note that C_l and C_r are implicitly functions of the displacement field $u_z(t, x)$, with $C_l(u_z=0) = C_r(u_z=0) \equiv C_b$.

Introducing creation/annihilation operators for both the LC circuits and the elastic strip modes, and expanding the LC circuit resonant frequencies to first order in the strip transverse displacement field, the total Hamiltonian of the LC system and acoustic phonon bath reduces to the standard optomechanical Hamiltonian

$$\mathcal{H} = \sum_{k=1}^2 \left[\hbar \Omega_b \left(a_k^\dagger a_k + \frac{1}{2} \right) + \sum_{j=1}^{\infty} \hbar g_{k,j} \left(a_k^\dagger a_k + \frac{1}{2} \right) (b_j + b_j^\dagger) \right] + \sum_{j=1}^{\infty} \hbar \omega_j \left(b_j^\dagger b_j + \frac{1}{2} \right), \quad (3)$$

where a_k (a_k^\dagger) are the annihilation (creation) operators for the LC oscillators with bare frequency $\Omega_b = 1/\sqrt{C_b L}$, with the subscript $k = 1, 2$ denoting the left, right LC oscillator, and b_j (b_j^\dagger) are the annihilation (creation) operators for the elastic strip modes of frequency $\omega_j = \pi j \sqrt{\frac{F}{2mL}}$ with $m = \rho_m W T L / 2$ the effective mass of the modes. The coupling strength between each LC oscillator and

the elastic strip modes is given approximately by [29]

$$g_{1(2),j} = -\frac{\Omega_b}{2d} \left(\frac{\hbar}{2m\omega_j} \right)^{1/2} \text{sinc} \left(\frac{\omega_j}{\omega_u} \right) \times \sin \left(\frac{\pi j}{L} \times \frac{L \mp D \mp \Delta L}{2} \right), \quad (4)$$

where $\text{sinc } x := \overline{\sin(x)}/x$ and the cut-off frequency is $\omega_u = \frac{2}{\Delta L} \sqrt{\frac{FL}{2m}}$, corresponding to the characteristic wavelength $\pi \Delta L$, which is of the same order as the capacitor size; the decaying sinc function results in the coupling to higher frequency modes approaching zero asymptotically for $\omega_j \gg \omega_c$. The term $\frac{L \mp D \mp \Delta L}{2}$ inside the sine function denotes the x coordinate for the center of the left (-) and right (+) capacitors, respectively.

We note, however, that with the mode frequency ω_j dependence of the above given coupling strength $g_{j,k}$, there is no ultraviolet (UV) divergence when taking the limit $\omega_u \rightarrow +\infty$ in the determination of the quantum dynamics of the LC oscillator systems given below; this is a consequence of the effective one dimensional nature of the elastic strip [29]. Since the capacitor length ΔL is assumed to be much smaller than the length L of the strip, we shall therefore take the ‘point-like’ UV limit for the capacitors by dropping the upper cut-off regulating sinc function and setting $\Delta L = 0$ for the coupling strength in the following. This then allows closed form analytical solutions for the quantum dynamics.

Assuming that the LC oscillators and the elastic strip state are prepared initially in a product state with the latter in a thermal state, the time evolution of the reduced oscillator system density matrix expanded in the Fock state basis can be expressed as follows [29]:

$$\begin{aligned} \rho_{n_1 n_2, n'_1 n'_2}(t) &= \exp \left(-it \Omega_b (n_1 + n_2 - n'_1 - n'_2) \right) \\ &+ ip_1(t) \left[(n_1 + n'_1 + 1)(n_1 - n'_1) + (n_2 + n'_2 + 1)(n_2 - n'_2) \right] \\ &+ ip_2(t) \left[(n_1 + n'_1 + 1)(n_2 - n'_2) + (n_2 + n'_2 + 1)(n_1 - n'_1) \right] \\ &- d_1(t) \left[(n_1 - n'_1)^2 + (n_2 - n'_2)^2 \right] \\ &- d_2(t) (n_1 - n'_1)(n_2 - n'_2) \rho_{n_1 n_2, n'_1 n'_2}(0), \end{aligned} \quad (5)$$

where the time-dependent terms are given, respectively,

by

$$p_1(t) = \lambda \left(\frac{\pi^2 \tau}{6} - \tau \operatorname{Re}[\operatorname{Li}_2(-e^{i\sigma})] + \operatorname{Im} \left[\frac{1}{2} \operatorname{Li}_3(-e^{i(\tau+\sigma)}) + \frac{1}{2} \operatorname{Li}_3(-e^{i(\tau-\sigma)}) - \operatorname{Li}_3(e^{i\tau}) \right] \right), \quad (6a)$$

$$p_2(t) = \lambda \left(\frac{\pi^2 \tau}{12} + \tau \operatorname{Re}[\operatorname{Li}_2(e^{i\sigma})] - \operatorname{Im} \left[\operatorname{Li}_3(-e^{-i\tau}) + \frac{1}{2} \operatorname{Li}_3(e^{i(\tau-\sigma)}) + \frac{1}{2} \operatorname{Li}_3(e^{i(\tau+\sigma)}) \right] \right), \quad (6b)$$

$$d_1(t) = \sum_{j=1}^{\infty} \frac{1 - \cos(\omega_j t)}{\omega_j^2} g_{1,j}^2 \coth \left(\frac{\beta \hbar}{2} \omega_j \right), \quad (6c)$$

$$d_2(t) = 2 \sum_{j=1}^{\infty} \frac{1 - \cos(\omega_j t)}{\omega_j^2} g_{1,j} g_{2,j} \coth \left(\frac{\beta \hbar}{2} \omega_j \right), \quad (6d)$$

in which $\beta^{-1} = k_B T$, with k_B Boltzmann's constant and T the bath temperature. The dimensionless numerical constant $\lambda = \frac{\Omega_b^2 \hbar}{16 d^2 m \omega_1^3}$, and $\operatorname{Li}_s(\cdot)$ is the polylogarithm function of order s . Note that we have also introduced the notations for the dimensionless time: $\tau = \omega_1 t$, and the scaled distance ratio: $\sigma = \pi D/L$ in the above expressions. Equation (5) neglects any influence due to environments that couple directly to the LC oscillators and the elastic strip systems, since we seek here to understand purely the effects of the optomechanically coupled, long stripline alone on the LC oscillators' reduced quantum dynamics.

We now make several observations based on the form of Eq. (5) about the LC oscillators' reduced system dynamics. The first term in the argument of the exponential in Eq. (5) is just the free evolution of the system. The $p_1(t)$ and $d_1(t)$ terms correspond to environment induced renormalization and dephasing respectively of the individual LC oscillators, while the $p_2(t)$ and $d_2(t)$ terms encode the effective environment induced mutual dynamics between the two LC oscillators. In particular, we have competing processes here where a non-zero mutual phase term $p_2(t)$ can render the LC oscillators' reduced density matrix non-separable, i.e., we have entanglement generation between the two LC oscillator subsystems, while on the other hand, the real dephasing terms $d_1(t)$ and $d_2(t)$ serve to counter entanglement generation. However, since both the $d_1(t)$ and $d_2(t)$ terms contain the oscillating factor $1 - \cos(\omega_j t)$, in which the harmonic mechanical modes frequencies are equally-spaced, these two terms completely vanish at times $t = 2\pi j/\omega_1, j = 0, 1, 2, \dots$. This periodic, full rephasing phenomenon is crucial to the analysis of the entanglement generation as we will see below; in particular, it allows for periodic time windows in which to probe the generated entanglement, of course neglecting decoherence effects due to intrinsic environments of the LC oscillators and elastic strip. We note that this full rephasing phenomenon is a consequence of the one dimensional nature of the long elastic strip with equally spaced vibrational modes. Only partial rephasing

will occur for two dimensional, elastic membranes with non equally spaced vibrational modes [29].

Causality.— Before we discuss our main results on the entanglement generation dynamics, it is of interest to first analyze the causal aspects of the model dynamics, which is often absent in the literature concerning entanglement generation between spatially separated local subsystems. Although the elastic displacement (phonon) field u_z does not obey the Lorentz symmetry, its Hamiltonian (1) takes the same form as a relativistic massless quantum field in the lab frame, with the speed of light replaced by the acoustic sound (phonon) speed $v_{\text{ph}} = \sqrt{\frac{FL}{2m}}$. Causality then requires that the physical state of one LC circuit will not be changed by the presence of the other within the time that it takes for phonons to travel the separation distance between the two capacitors: $\Delta t = \frac{D}{v_{\text{ph}}} = \sqrt{\frac{2m}{FL}} D$. Performing a partial trace over one of the LC oscillator subsystem's density matrix, one can easily see from Eq. (5) that the influence of one LC oscillator on the other is only through the $p_2(t)$ term. Considering the following inequalities for τ and σ : $\tau < \sigma$ (corresponding to $t < \Delta t$) and $\sigma < \pi$ (corresponding to $D < L$), $p_2(t)$ in Eq. (6b) can be rewritten as a combination of Bernoulli polynomials that are verified to vanish exactly, thus fulfilling the causality requirement. We stress that such a causally consistent result can only be obtained by an exact, field theoretic treatment of the environment [30] (i.e., taking account of the position-dependent coupling between system and bath and summing over all environmental bath degrees of freedom); if one approximately truncates to a finite number of field modes in the sum, causality is violated. For example, as we show in Fig. 2, a strongly acausal result is obtained with only the contribution from the lowest, fundamental frequency mode of the elastic strip taken into account. By including more modes in the sum, the induced phase term $p_2(t)$ approaches its exact analytical expression, but nevertheless remains acausal.

Zero temperature entanglement.— We now discuss the entanglement dynamics in the model. Since the tensor product of the Fock state is an eigenstate of the Hamiltonian (5), it is apparent that to entangle two initially separable subsystems, one has to prepare both of them in a superposition of Fock states. For simplicity, we shall consider the superposition of zero photon and single photon states for each LC circuit in the following: $|\psi(0)\rangle = \frac{1}{2} (|0\rangle_l + |1\rangle_l) \otimes (|0\rangle_r + |1\rangle_r)$, with the labels l (r) denoting the left (right) LC circuit; since the photon number cannot change, each circuit LC circuit then functions effectively as a two-level system.

We shall first focus on the zero temperature limit of the phonon field (corresponding to the vacuum field state of the strip). Despite it being a challenge to realize given the presence of low frequency modes of the long elastic strip, the zero temperature limit allows analytical expressions

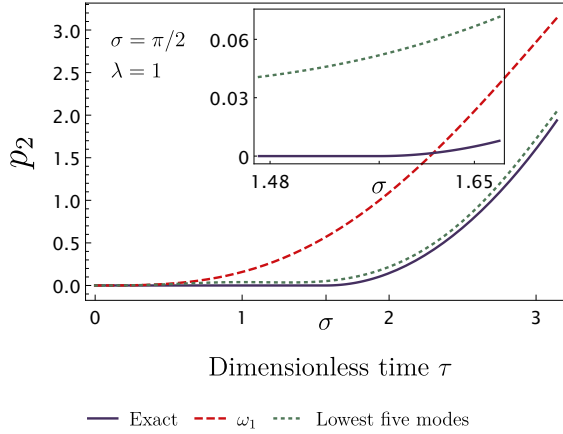


FIG. 2. The environment induced mutual phase term $p_2(t)$ plotted as a function of dimensionless time $\tau = \omega_1 t$. The constant $\lambda = 1$ and $\sigma = \pi/2$ (corresponding to the LC circuits' separation $D = L/2$). Both the exact analytical expression (6b) (solid line) and finite mode sum approximations are shown for comparison: the contribution from the lowest, fundamental mode ω_1 only (dashed line) and the contribution obtained by summing over the lowest five elastic frequency modes only (dotted line). The inset gives the zoomed in plot for p_2 close to $t = \sigma$.

for the dephasing terms and yields important information about the competition between dephasing and entanglement generation. Taking the limit $\beta \rightarrow +\infty$ in Eqs. (6c) and (6d), we have

$$d_1(t) = \lambda \left(\text{Re} \left[\frac{1}{2} \text{Li}_3(-e^{-i(\tau-\sigma)}) + \frac{1}{2} \text{Li}_3(-e^{i(\tau+\sigma)}) - \text{Li}_3(e^{i\tau}) - \text{Li}_3(-e^{i\sigma}) + \zeta(3) \right] \right), \quad (7a)$$

$$d_2(t) = 2\lambda \left(\text{Re} \left[\text{Li}_3(-e^{-i\tau}) + \text{Li}_3(e^{i\sigma}) - \frac{1}{2} \text{Li}_3(e^{i(\tau-\sigma)}) - \frac{1}{2} \text{Li}_3(e^{i(\tau+\sigma)}) + \frac{3}{4} \zeta(3) \right] \right), \quad (7b)$$

where ζ is the Euler–Riemann zeta function. To determine whether the system is entangled, we utilize the logarithmic negativity [31]: $E_N(\rho) \equiv \log_2(\|\rho^{\Gamma_t}\|)$ as our entanglement measure, where ρ^{Γ_t} is the partial transpose of ρ with respect to the left subsystem and $\|\cdot\|$ denotes the trace norm. A positive value of E_N implies the presence of entanglement in our (two-level) bipartite system.

With the full time evolution of the system density matrix given by Eq. (5) and the calculated time dependent terms $p_1(t)$, $p_2(t)$, $d_1(t)$, and $d_2(t)$, we obtain the logarithmic negativity E_N as a function of the dimensionless time $\tau = \omega_1 t$ shown in Fig. 3. It can be seen from Fig. 3 that the entanglement dynamics is sensitive to the value of the numerical constant λ , with several features in the

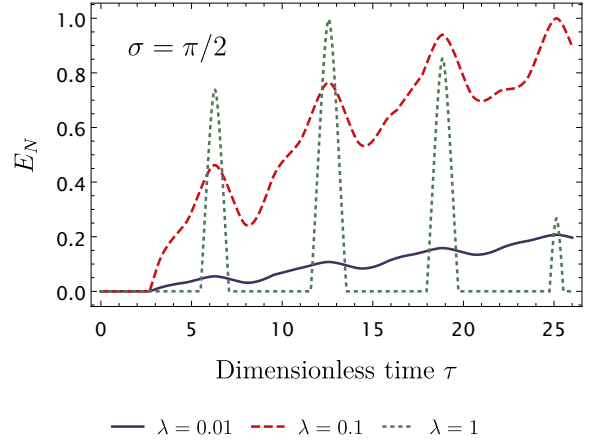


FIG. 3. Logarithmic negativity plotted as a function of dimensionless time $\tau = \omega_1 t$ with different values of the numerical constant λ . The parameter $\sigma = \pi/2$ (corresponding to the LC circuits' separation $D = L/2$)

time dependence noted as follows: (1) For the parameters considered here, the entanglement can only build up some time later than $t = \Delta t$ (corresponding to $\tau = \sigma$), the time required for phonons to travel the separation distance D between the subsystems. Such a result means that entangled states can only be generated when the two subsystems are ‘timelike’ with respect to the phonon speed v_{ph} , which is the combined consequence of causality and the effect of zero temperature dephasing; although the environment induced phase term $p_2(t)$ starts to build up immediately after $t = \Delta t$ (Fig. 2), some additional time may be required in order to overcome the dephasing in order for entanglement to develop between the two subsystems. In particular, entanglement would otherwise immediately build up after $t = \Delta t$ in the artificial situation where the dephasing is suppressed [i.e., $d_1(t) = d_2(t) = 0$]. (2) E_N is a local maximum at $\tau = 2j\pi$, $j = 1, 2, 3, \dots$, corresponding to when both $d_1(t)$ and $d_2(t)$ vanish exactly, as noted previously. Furthermore, depending on the value of the numerical constant λ , E_N can reach its upper bound value 1 for the two-level bipartite system, signaling a maximally entangled system state. (3) With the periodic vanishing of the dephasing terms, the maximally entangled state can always be generated regardless of the separation distance between the LC circuits; a larger separation distance only results in a longer time for the entanglement to build up. (4) Entanglement at zero temperature clearly demonstrates the necessity of the elastic strip displacement field being quantum; since there is no energy exchanged between the LC circuit system and the elastic displacement field, if the latter were to be modeled classically, then the vacuum state of the field would correspond to it being at absolute rest (i.e., undisplaced)

with no communication channel between the two LC circuit systems.

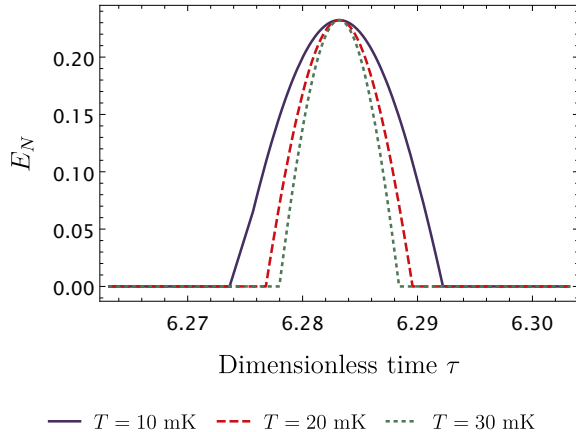


FIG. 4. Logarithmic negativity plotted as a function of dimensionless time $\tau = \omega_1 t$ for different phonon field temperatures; the utilized parameters of the model are discussed in the text, and correspond to the numerical constant $\lambda \approx 0.045$.

Finite temperature entanglement and experimental considerations.— We now shift our focus to more realistic, finite temperature scenarios, where the entanglement generation can be strongly suppressed due to the much more rapid thermal dephasing as compared with the zero temperature limit. However, as we have seen previously, the entanglement can nonetheless be present in the system around the times $\tau = 2j\pi, j = 1, 2, 3, \dots$ when there is full rephasing (neglecting the other circuit and elastic strip decohering environments). In order to quantitatively investigate the entanglement dynamics, we assume some example parameters for the model related to actual experimental devices. In particular, For the elastic strip, we adopt the silicon nitride vibrating string parameters from Ref. [32]: $\rho_m = 10^3 \text{ kg/m}^3$, $F = 10^{-5} \text{ N}$, $W = 1 \text{ }\mu\text{m}$, $T = 0.1 \text{ }\mu\text{m}$; However, we assume a much longer length $L = 2 \text{ cm}$ than that considered in Ref. [32] ($\approx 60 \text{ }\mu\text{m}$). For the LC oscillators, we adopt typical superconducting microwave LC circuit parameters with $\Delta L = 1 \text{ }\mu\text{m}$, $d = 0.1 \text{ }\mu\text{m}$, and the circuit mode frequency of $\Omega/(2\pi) = 15 \text{ GHz}$. The separation distance between the capacitors is taken to be $D = 1 \text{ cm}$.

Using the above given parameters, we obtain the numerical results shown in Fig. 4 for the logarithmic negativity plotted around $\tau = 2\pi$, with different example temperatures achievable in a dilution refrigerator. Note that the amount of entanglement at $\tau = 2\pi$ when there is full rephasing (corresponding to $t \sim 126 \text{ }\mu\text{s}$) is not changed by the environment temperature. Instead, increasing the temperature narrows time window (corresponding to a width around 150 ns for $t = 30 \text{ mK}$ in Fig. 4) during

which the LC circuits system is entangled.

In order to experimentally probe the entanglement within the system, the initial and final LC systems' state may for example be prepared and measured by coupling the LC circuits to driven nonlinear Josephson phase qubits [33]. With respect to the unavoidable LC circuit environments, we note that relaxation and dephasing times from around a hundred to a few hundred microseconds have been reported for superconducting circuits [34–37], thus allowing for the possibility to measure the first entanglement generation peak captured by the logarithmic negativity using available circuit QED experimental methods [38].

Discussion.— In summary, we have investigated in detail the entanglement dynamics for two LC oscillators coupled to a long elastic strip. Exact solutions for the quantum time evolution of the oscillators were obtained, and the causality of the quantum dynamics analysed.

Since the optomechanical interaction bears some similarities with the matter-graviton interaction $H_I \sim T^{\mu\nu}(\phi)h_{\mu\nu}$, with $T^{\mu\nu}(\phi)$ the scalar field energy-momentum tensor and $h_{\mu\nu}$ the gravitational metric perturbation from flat spacetime, our model might serve as a gravitational entanglement generation analogue for informing about recent proposals to observe quantum gravity effects at low energies [39, 40]. In these proposals, only the effective Newtonian gravitational interaction potential was considered for inducing entanglement between an initial product of matter superposition states, serving as an indirect witness for quantum gravity. If gravity is indeed a quantum field entity, then the Newtonian potential corresponds to the nonrelativistic, action at a distance limit of the effective field theory description of the graviton. In this regard, our model analog demonstrates explicitly how the quantum phonon field is responsible for the entanglement generation in the system, with retardation effects exactly taken into account.

Finally, with potential applications to quantum information processing in mind, we note that it should be straightforward to extend our model to multiple LC circuits and investigate possible multipartite entanglement generation via the optomechanical interaction with a common, thermal elastic wave environment.

We thank Shadi Ali Ahmad and Sougato Bose for helpful discussions. This work is supported by a Dartmouth Teaching Fellowship and by the NSF under grant no. PHY-2011382.

* qidong.xu.gr@dartmouth.edu

† miles.p.blencowe@dartmouth.edu

[1] W. H. Zurek, Physical Review D **26**, 1862 (1982).

[2] E. Joos and H. D. Zeh, Zeitschrift für Physik B Condensed Matter **59**, 223 (1985).

[3] W. H. Zurek, Physics Today **44**, 36 (1991).

- [4] M. P. Blencowe, *Physical Review Letters* **111**, 021302 (2013).
- [5] D. Braun, *Physical Review Letters* **89**, 277901 (2002).
- [6] F. Benatti, R. Floreanini, and M. Piani, *Physical Review Letters* **91**, 070402 (2003).
- [7] R. Romano and D. D'Alessandro, *Physical Review Letters* **97**, 080402 (2006).
- [8] A. Ferreira, A. Guerreiro, and V. Vedral, *Physical Review Letters* **96**, 060407 (2006).
- [9] L. Contreras-Pulido and R. Aguado, *Physical Review B* **77**, 155420 (2008).
- [10] J. P. Paz and A. J. Roncaglia, *Physical Review Letters* **100**, 220401 (2008).
- [11] D. P. McCutcheon, A. Nazir, S. Bose, and A. J. Fisher, *Physical Review A* **80**, 022337 (2009).
- [12] T. Zell, F. Queisser, and R. Klesse, *Physical Review Letters* **102**, 160501 (2009).
- [13] F. Galve, L. A. Pachón, and D. Zueco, *Physical Review Letters* **105**, 180501 (2010).
- [14] P. Eastham, P. Kirton, H. Cammack, B. Lovett, and J. Keeling, *Physical Review A* **94**, 012110 (2016).
- [15] L.-Z. Hu, Z.-X. Man, and Y.-J. Xia, *Quantum Information Processing* **17**, 1 (2018).
- [16] A. Retzker, J. I. Cirac, and B. Reznik, *Physical Review Letters* **94**, 050504 (2005).
- [17] C. Sabín, J. J. García-Ripoll, E. Solano, and J. León, *Physical Review B* **81**, 184501 (2010).
- [18] C. Sabín, B. Peropadre, M. del Rey, and E. Martín-Martínez, *Physical Review Letters* **109**, 033602 (2012).
- [19] M. Cattaneo, G. L. Giorgi, S. Maniscalco, G. S. Paroanu, and R. Zambrini, *Annalen der Physik* **533**, 2100038 (2021).
- [20] L. Aolita, F. De Melo, and L. Davidovich, *Reports on Progress in Physics* **78**, 042001 (2015).
- [21] W. G. Unruh, *Physical Review D* **14**, 870 (1976).
- [22] B. S. DeWitt, "Quantum gravity: the new synthesis," in *General Relativity: An Einstein Centenary Survey* (Cambridge University Press, 1979) pp. 680–745.
- [23] B. Reznik, *Foundations of Physics* **33**, 167 (2003).
- [24] B. Reznik, A. Retzker, and J. Silman, *Physical Review A* **71**, 042104 (2005).
- [25] E. Martín-Martínez, E. G. Brown, W. Donnelly, and A. Kempf, *Physical Review A* **88**, 052310 (2013).
- [26] G. Salton, R. B. Mann, and N. C. Menicucci, *New Journal of Physics* **17**, 035001 (2015).
- [27] S.-Y. Lin and B. L. Hu, *Physical Review D* **79**, 085020 (2009).
- [28] E. G. Brown, E. Martín-Martínez, N. C. Menicucci, and R. B. Mann, *Physical Review D* **87**, 084062 (2013).
- [29] Q. Xu and M. P. Blencowe, arXiv preprint: 2109.05338 (2021).
- [30] D. M. Benincasa, L. Borsten, M. Buck, and F. Dowker, *Classical and Quantum Gravity* **31**, 075007 (2014).
- [31] G. Vidal and R. F. Werner, *Physical Review A* **65**, 032314 (2002).
- [32] R. Schilling, H. Schütz, A. Ghadimi, V. Sudhir, D. J. Wilson, and T. J. Kippenberg, *Physical Review Applied* **5**, 054019 (2016).
- [33] M. Hofheinz *et al.*, *Nature* **459**, 546 (2009).
- [34] M. Reagor *et al.*, *Physical Review B* **94**, 014506 (2016).
- [35] A. Nersisyan *et al.*, in *2019 IEEE International Electron Devices Meeting (IEDM)* (IEEE, San Francisco, CA, USA, 2019) pp. 31.1.1–31.1.4.
- [36] K. X. Wei, I. Lauer, S. Srinivasan, N. Sundaresan, D. T. McClure, D. Toyli, D. C. McKay, J. M. Gambetta, and S. Sheldon, *Physical Review A* **101**, 032343 (2020).
- [37] H. Zhang, S. Chakram, T. Roy, N. Earnest, Y. Lu, Z. Huang, D. Weiss, J. Koch, and D. I. Schuster, *Physical Review X* **11**, 011010 (2021).
- [38] A. Blais, A. L. Grimsmo, S. Girvin, and A. Wallraff, *Reviews of Modern Physics* **93**, 025005 (2021).
- [39] S. Bose, A. Mazumdar, G. W. Morley, H. Ulbricht, M. Toroš, M. Paternostro, A. A. Geraci, P. F. Barker, M. Kim, and G. Milburn, *Physical Review Letters* **119**, 240401 (2017).
- [40] C. Marletto and V. Vedral, *Physical Review Letters* **119**, 240402 (2017).